TRABECULAR TEXTURE ANALYSIS IN DENTAL CBCT BY MULTI-ROI MULTI-FEATURE FUSION

Peiyi Li[1], Xiong Yang[1,2], Fangfang Xie[3], Jie Yang[3], Erkang Cheng[1], Vasileios Megalooikonomou[1], Yong Xu[2], Haibin Ling[1]

[1] Department of Computer and Information Sciences, Temple University, Philadelphia, USA

[2] School of Computer Science and Engineering, South China University of Technology, Guangzhou, China

[3] Division of Oral and Maxillofacial Radiology, School of Dentistry, Temple University, Philadelphia, USA

ABSTRACT

Variations in trabecular bone texture are known to be correlated with bone diseases, such as osteoporosis. In this paper we propose a multi-feature multi-ROI (MFMR) approach for analyzing trabecular patterns inside the oral cavity using cone beam computed tomography (CBCT) volumes. For each dental CBCT volume, a set of features including fractal dimension, multi-fractal spectrum and gradient based features are extracted from eight regions-of-interest (ROI) to address the low image quality of trabecular patterns. Then, we use generalized multi-kernel learning (GMKL) to effectively fuse these features for distinguishing trabecular patterns from different groups. To validate the proposed method, we apply it to distinguish trabecular patterns from different gender-age groups. On a dataset containing dental CBCT volumes from 96 subjects, divided into gender-age subgroups, our approach achieves 96.1% average classification rate, which greatly outperforms approaches without the feature fusion.

Index Terms— Trabecular structure, multi-fractal spectrum, generalized multi-kernel learning.

1. INTRODUCTION

Variations in trabecular bone textures are known to be correlated closely to bone density change and therefore can be potentially used to aid the analysis of bone diseases such as osteoporosis. In the past few decades, analysis of trabecular bone structure has been presented in a variety of biomedical contexts. The importance of trabecular perforations in the development of osteoporosis has been introduced in [4]. Eriksen [2] explains the relation between the profound disintegration of the trabecular bone network and certain bone diseases [1]. This relation is also proved by another multicenter trial on trabecular bone which is to assess the effect of involutional osteoporosis on it [3]. Moreover, studies have shown that the change of the trabecular bone texture in iliac can foresee osteoporosis based on its surface texture, volume and thickness; and such pattern change can also distinguish bones structures of young people from those of seniors [4].

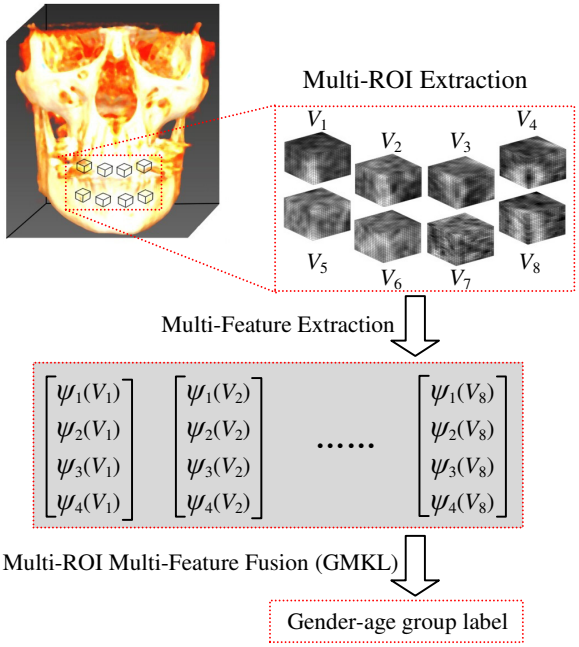

Fig. 1: A 3D CBCT volume (top left), extracted trabecular ROIs (top right), hybrid features extracted from these ROIs (middle), and GMKL-based gender-age classification (bottom).

Trabecular bone textures inside the oral cavity have been studied for osteoporosis analysis [11]. Previous studies, however, focus on validating the correlation between the trabecular pattern change and bone density loss. No effective dental image-based osteoporosis prescreening method has been reported so far.

In this paper we propose using 3D cone beam computed tomography (CBCT) for analyzing trabecular textures inside the oral cavity. In particular, for a given 3D dental CBCT, we first crop regions of interest (ROIs) containing trabecular structures and then apply texture analysis on these ROIs. An illustration of such trabecular bone ROIs is shown in Fig. 1. Compared with 2D radiographs, CBCT volumes provide rich 3D information containing important structure information of trabecular patterns. However, since the trabecular struts are usually much thinner than CBCT voxels,

it is hard to trace the structure directly. In addition, the possible distortion of CT values in CBCT reconstruction may bring some noise.

To address the above issues, we propose a robust texture analysis approach. First, instead of using simple texture descriptions from a single ROI, we propose a multi-feature multi-ROI (MFMR) representation. In particular, we use a set of features including fractal dimension, multi-fractal spectrum (MFS) and gradient based features extracted from eight different ROIs in the oral cavity. Then, we fuse these features in the generalized multi-kernel learning (GMKL) framework, which builds an effective classifier to distinguish trabecular patterns from different groups. Figure 1 summarizes the proposed approach.

The evaluation is conducted on a dataset containing CBCT volumes from 96 subjects in four gender-age subgroups. The experimental results demonstrate clearly the effectiveness of the feature fusing strategy and the MKL classifier in distinguishing trabecular patterns from different subgroups.

In the rest of the paper, Sec. 2 describes the proposed methodological framework; Sec. 3 gives the experimental results; and Sec. 4 concludes the paper.

2. METHODOLOGY

2.1. Problem Formulation

We aim to investigate the feasibility of using dental CBCT for the study of bone density loss. While it has been shown that intensity values in 2D radiographs and CT volumes are correlated directly to bone density [4][11], such correlation is less obvious for CBCT due to the distortion in CBCT reconstruction mentioned before. Our conjecture is that, although the measurement in CBCT may not be reliable for bone density estimation, the texture patterns are still useful for bone density loss study.

We have developed a framework for classifying trabecular patterns using machine learning tools. In particular, we first extract various types of features from multiple ROIs, and then fuse the features using MKL.

Note that, while it would be ideal to conduct the study on CBCT datasets with known bone mass density (BMD) status, i.e., measured by the gold standard, it is practically very hard to collect such datasets due to the high cost involved. Alternatively, we are taking advantage of the fact that BMD is closely correlated with gender and age [4].

In [4], it shows that the reduction in trabecular bone volume observed in normal subjects with increasing age is mainly due to a reduction in plate density. On the other hand, the further reduction in trabecular bone volume observed in patients with osteoporotic vertebral fracture is also mainly due to a further reduction in plate density. This study [4] indicates that gender-age-related bone loss in thickness is in a similar way that osteoporosis takes effect on trabecular bone structure. Consequently, approaches to distinguish trabecular patterns from different gender-age subgroups have great potentials to be extended for osteoporosis prescreening by trabecular pattern analysis.

Motivated by this study, we use a dataset involving subjects having normal BMD status from different gender-age subgroups. Our problem is then formulated as using trabecular texture analysis to distinguish different gender-age subgroups.

2.2. Multiple Dental ROIs

Benefiting from the fact that trabecular patterns are distributed in various places in the oral cavity, we integrate information from multiple ROIs for robustness.

For a dental CBCT volume denoted as S, we use eight ROIs including areas apical to the maxillary left and right premolars, mandibular left and right lateral incisors and first molars, left and right condyles. For each ROI, a cube of size 19×19×19 containing trabecular structure is cropped. We denote the eight trabecular cubes as $\boldsymbol{V}=\{V_i, i=1,\ldots,8\}$.

2.3. Feature Descriptors

We extract different types of 3D texture descriptors from each trabecular cube. Let $\boldsymbol{S}=\{S^{(k)}: k=1,...,96\}$ be our sample set containing 96 volumes, each sample $S^{(k)}$ has 8 ROIs $\{V_i^{(k)}: i=1,...,8\}$ defined above. Four types of features, denoted as ψ_c, $c=1,...,4$, are extracted from each ROI. Collecting all these features together, our proposed 3D texture features for a single sample $S^{(k)}$ are denoted as

$$\psi(S^{(k)})=\{\psi_c(V_i^{(k)}): i=1,...,8; c=1,...,4\}.$$

The four different features are described below.

Multi-fractal spectrum (MFS). The first type of feature (ψ_1) is the multi-fractal spectrum (MFS) which has been recently used successfully for general texture classification [6][9]. Motivated by the work in [6], we extend MFS from the 2D case to 3D for describing texture patterns.

Given a ROI cube V, MFS of V is a sequence of fractal dimensions (FD), which are calculated on a partition of the support of V. Specifically, the set voxels in V is first partitioned as a disjoint point set $\{\Lambda_1, \Lambda_2, \ldots, \Lambda_8\}$ according to voxel intensities. Then FD for each set is estimated using the box counting algorithm [16]. Specifically, let the space R^3 be covered by a mesh of three-dimensional cubes with side length r (i.e., r-mesh) and a counting function $c(\Lambda, r)$ is defined as the number of r-mesh hyper cubes that intersect Λ. Then the box-counting fractal dimension $d(\Lambda)$ is defined as

$$d(\Lambda)=\lim_{r\to 0}\frac{\log c(\Lambda,r)}{-\log r}.$$

Finally, the MFS for ROI V is defined as

$$\psi_1(V)=(d(\Lambda_1), d(\Lambda_2), \ldots, d(\Lambda_8)).$$

Fractal Dimension (FD). The second type of feature (ψ_2) is the fractal dimension of the whole patch, which captures the global density pattern of trabecular texture. For a ROI V, we first threshold on its intensity to get point set Λ, then calculate $\psi_2(\Lambda)$ according to the box counting algorithm described above.

Gradient Magnitude (GM). The third type of feature (ψ_3) is Gradient Magnitude (GM) which captures the strength of edge responses at voxels.

3D Histogram of Oriented Gradient (3D HOG). The fourth type of feature (ψ_4) is the histogram of 3D oriented gradient (3D HOG). This is extended from the 2D HOG that has been shown to be very robust in capturing discriminative information in many pattern recognition applications [15]. In particular, for a cube V, we define

$$\psi_4(V)=(h_1, h_2, \ldots, h_{20}),$$

where h_i counts the number of voxels whose gradient orientation fall in the i^{th} gradient orientation bin.

2.4. Generalized Multi Kernel Learning

We formulate our problem as gender-age classification. Let us denote our training set as $\{S^{(k)}, y^{(k)}\}$, where $S^{(k)}$ is a CBCT volume and $y^{(k)}$ its label (i.e., the gender-age group S_i belongs to). For each sample $S^{(k)}$, we denote its texture vector as

$$\boldsymbol{x}^{(k)}= \psi(S^{(k)})=\{ \boldsymbol{x}^{(k)}_{i,c}= \psi_c(V_i^{(k)}):\ i=1,...,8;\ c=1,...,4\}.$$

The training set is now converted to $\{\boldsymbol{x}^{(k)}, y^{(k)}\}$. We use the generalized multi-kernel learning (GMKL) to fuse the multi-ROI multi-feature information. By treating each ROI-feature component (i.e. $\boldsymbol{x}^{(k)}_{i,c}$) with a kernel, GMKL provides a natural and effective means to fuse multi-ROI multi-feature information.

The classic multi-kernel learning (MKL) assumes the linear combination of kernels in the form of

$$K(x_i, x_j) = \sum_k d_k K_k(x_i, x_j),$$

where K_k denotes basis kernels. GMKL breaks the linearity limitation by allowing non-linear kernel combinations such as

$$K(x_i, x_j) = \prod_l K_l(x_i, x_j)\cdot$$

In our study, we use the fusing strategy

$$K_d(x_i, x_j) = e^{-\sum_m d_m x_i^t A_m x_j},$$

combined with a sparsity promoting regularizer on the kernel combination coefficient vector $\mathbf{d}$. To learn the GMKL model, given the training dataset$\{\boldsymbol{x}^{(k)}, y^{(k)}\}$, we use the MKL formulation in [12]

$$\min_{\mathbf{w},b,\mathbf{d}} \frac{1}{2}\mathbf{w}^t\mathbf{w} + \sum_{i,r,t} l(y^{(i)}, f(\mathbf{x}^{(i)})) + r(\mathbf{d})$$

subject to $\mathbf{d}\geq 0$,

where $\mathbf{w}$, $\mathbf{d}$ and b are model parameters to be learned, $l(.)$ the standard lost function, and $r(.)$ the regularizer. We use the l_1 regularization $r(\mathbf{d}) = \sigma^t\mathbf{d}$, where σ is the variation to encourage sparsity.

For the above optimization problem, the standard procedure [17] is used to reformulate the primal as a nested two step optimization. We use the same final algorithmic framework given by [12].

3. EXPERIMENTS

3.1. Experimental Data

In order to evaluate the proposed method, we used a dataset containing 96 3D-CBCT volumes from four gender-age subgroups: female younger (FY) than 40 years, female older (FO) than 40 years, male younger (MY) than 40 years, male older (MO) than 40 years. Samples(patients) are all of normal BMD. Table 1 gives a summary of the dataset. Each CBCT scan was obtained by using an i-Cat machine (Imaging Science International, Inc., Hatfield, PA, USA) with a 400x400 matrix taken at 0.3 mm slice thickness, and in average each volume has 327 slices.

Number of samples	Female	Male
Less than 40 years old	13	8
More than 40 years old	48	27

Table 1: Trabecular CBCT dataset used in this study

For each volume, a dentist manually cropped the eight ROIs requested in the proposed approach. Some examples of trabecular cubes are shown in Figure 1.

3.2. Experimental Configuration

We use a comparison experiment to investigate the proposed GMKL-based multi-feature multi-ROI fusion. From the four gender-age groups, six pairs of subgroups are generated which require six classification tasks. For each task, we evaluate the proposed approaches with several baselines described below.

We evaluate the proposed approach in two aspects. First, we study the effectiveness of using GMKL for feature fusion. For this purpose, we include the standard support vector machine (SVM) as a baseline. Specifically, all features from all ROIs are concatenated into a long feature vector as input. Then, the SVM is trained on the input with a single kernel. By contrast, the proposed algorithm fuses all features by fusing 32 kernels using GMKL.

Second, we compare the proposed approach with baselines that use only a single ROI with a single type of feature. There are 32 such baselines correspond to the combination of eight ROIs and four feature types. All the baselines use SVM with a single kernel. For example, each $S^{(k)}$ we can extract $\{\boldsymbol{x}^{(k)}_{i,c}: i=1,...,8; c=1,...,4\}$, which is totally 8 ROIs with 4 features each. So for comparison between two gender-age subgroups, instead of training a single classifier, we use SVM to train 32(=8x4) separate classifiers. We record the accuracies of all these classifiers. In this paper, due to the pages limit, we only report the average and the highest accuracies of all these classifiers.

In summary, we have four accuracies reported in our evaluation for each comparison between two gender-age subgroups. The accuracy of a single kernel SVM, the average accuracy of all 32 separate SVM classifiers, the highest accuracy among all 32 separate SVM, and the

accuracy of our proposed GMKL multi-ROI multi-feature fusion framework.

In the classification stage, we conducted a leave-one-out cross validation on the dataset with the selected features. In the training stage, we left one of the samples out and used the others for training a model. In the testing phase, we applied the learnt model to that leaved-out sample and recorded 1 for correct and 0 for incorrect. Then we repeated this procedure for every single sample. After the cross validation loop, by counting how many 1's among all samples, the average classification rates were reported.

3.3. Results

Table 2 shows the classification accuracies of different approaches described above, including the classic SVM classifier that takes all features as input, the SVM classifier for individual ROI-feature combinations (average and maximum performances), and the proposed GMKL-based solution.

Training Strategy	Accuracy on each gender-age subgroup (%)					
Gender-Age Group	FO&FY	FO&MO	FO&MY	FY&MO	FY&MY	MO&MY
SVM-average	78.81	63.53	85.54	67.94	60.71	76.43
SVM-max	86.89	65.33	89.29	80.00	71.43	80.00
SVM single-k	78.69	64.00	85.71	67.50	61.90	77.14
GMKL (proposed)	**96.72**	**98.00**	**98.21**	**91.25**	**95.24**	**97.14**

Table 2: Performance of different comparison experiments.

Illustrated in Table 2, experimental results are very promising considering that only 24 samples on the average are used for each gender-age subgroup. Our proposed feature fusing MKL classifier reaches an accuracy of 95% on most of the dataset subgroups. For a single-tooth single-feature SVM, even the highest accuracy still fall behind our proposed GMKL framework. We expect that more training samples will further boost the performance.

For the specific feature fusing strategy used in this framework, the results show that the traditional feature fusing method on SVM performs worse than our proposed GMKL fusing method. This indicates that for each single kind of feature descriptor, it will lose certain discriminative information which may be used for prescreening purposes. Only in the way which we consider the presence of both feature information and the correlations can minimize such loss. GMKL fusing strategy is the best choice.

4. CONCLUSION

We presented a study of trabecular texture analysis on dental CBCT by fusing multi-feature multi-ROI information in the multiple kernel learning framework. On a six gender-age group classification problem using a dental CBCT dataset containing 96 volumes, our method achieves a promising average accuracy of 96.1%, and significantly outperforms baseline methods.

Our results show that the combination of machine learning techniques and texture analysis can be used for trabecular pattern analysis. The results encourage future exploration using dental CBCT for aiding diagnosis of bone mass density related diseases.

ACKNOWLEDGEMENTS. This work was supported in part by NSF Research Grant IIS-0916624. The funding agency specifically disclaims responsibility for any analyses, interpretations and conclusions.

REFERENCES

[1] A.M. Parfitt, "Age related structural changes in trabecular and cortical bone. Cellular mechanisms and biomechanical consequences", *Calcif Tissue Int 36:S123-S128*, 1984.

[2] E.F. Eriksen, "Normal and Pathological Remodeling of Human Trabecular Bone: Three Dimensional Reconstruction of the Remodeling Sequence in Normals and in Metabolic Bone Disease", *Endocr Rev. 7(4):379-408*, 1986.

[3] J. Reeve, P.J. Meunier, et al, "Anabolic effect of human parathyroid hormone fragment on trabecular bone in involutional osteoporosis: a multicentre trial", *British Medical Journal 7*, 1980.

[4] A.M. Parfitt, C.H.E. Mathews, et al, "Relationships between Surface, Volume, and Thickness of Iliac Trabecular Bone in Aging and in Osteoporosis", *JCI, 72(4):1396-1409*, 1983.

[5] J.E. Aaron, N.B. Makins, and K. Sagreiya, "The Microanatomy of Trabecular Bone Loss in Normal Aging Men and Women", *CORR 215:260-271,* 1987.

[6] Y. Xu, X. Yang, H. Ling, and H. Ji, "A New Texture Descriptor Using Multifractal Analysis in Multi-orientation Wavelet Pyramid", *IEEE CVPR, 161-168*, 2010.

[7] R. Azencott, J. Wang, and L. Younes, "Texture Classification Using Windowed Fourier Filters", *IEEE TPAMI, 19(2)*, 1997.

[8] A. Teuner, O. Pichler, and B. J. Hosticka, "Unsupervised Texture Segmentation of Images Using Tuned Matched Gabor Filters", *IEEE Trans. Image Process, Vol. 4(6)*, 1995.

[9] L.M. Kaplan, "Extended Fractal Analysis for Texture Classification and Segmentation", *IEEE TPAMI. 8(11)*, 1999.

[10] S. Dudoit, J.P. Shaffer, and J.C. Boldrick, "Multiple Hypothesis Testing in Microarray Experiments", *Statistical Science, 18(1):71-103*, 2003.

[11] S.C. White, "Oral radiographic predictors of osteoporosis", *Dentomaxillofacial Radiology, 31(2):84-92*, 2002.

[12] M. Varma and B.R. Babu, "More generality in efficient multiple kernel learning", *ICML, 1065-1072*, 2009.

[13] J. Theiler, "Estimating Fractal Dimension", *Optical Society of America*, 1990.

[14] W.J. Yi, M.S. Heo, et al, "Direct measurement of trabecular bone anisotropy using directional fractal dimension and principal axes of inertia", *Oral Surg Oral Med Oral Pathol*, 2007.

[15] N. Dalal, B. Triggs, "Histograms of oriented gradients for human detection", *IEEE CVPR*, 2005.

[16] D. Russel, J. Hanson, E. Ott, "Dimension of strange attractors", *Phys. Rev. Lett. 45, 1175–1178*, 1980.

[17] O. Chapelle, V. Vapnik, O. Bousquet, & S. Mukherjee, "Choosing multiple parameters for Support Vector Machines", *Machine Learning*, 46, 131–159, 2001.